Tuijin Jishu/Journal of Propulsion Technology
ISSN: 1001-4055
Vol. 47 No. 01 (2026)

Microhardness Assessment of Magnesium Alloy after Powder Mixed Wire Electrical Discharge Machining and Hydroxyapatite Coating

Sunil Kumar[1*], Rajender Kumar[2], Puneet Katyal[1]

1Department of Mechanical Engineering, Guru Jambheshwar University of Science & Technology, Hisar, India
2Department of Basic Engineering, CCS Haryana Agricultural University, Hisar, India
**Email: Kumarsunil9712@gmail.com, *ORCID- 0000-0002-0455-7346*

Abstract: Magnesium (Mg) alloys, which have excellrnt biocompatibility and characteristics similar to bone, are ideal choices for temporary biodegradable othopedic implants. However, because of their low ductility and fast corrosion, their applicability in biological environments is currently limited. Surface properties can be altered by surface treatments such as coating, alloying, and mechanical working to make it application friendly. In this experimental study, ZE41A Mg alloy was processed with powder mixed wire electric discharge machining (PMWEDM) and hydroxyapatite (HA) coating, to analyse their effect on microstructure and micro-hardness. Surface microstructure of parent, PMWEDMed, and HA-coated samples was analyzed by using Field emission scanning electron microscopy (FE-SEM). The microhardness (MH) of these samples was determined using a Vickers micro-hardness tester before and after 14 days of immersion in simulated body fluid (SBF). The results show that PMWEDM and HA coating produced surfaces with higher MH. The post-immersion data show a loss of MH in all three types of Mg samples, which is attributed to sample degradation in SBF.

Keywords: *Microhardness; Hydroxyapatite; FE-SEM; Simulated Body Fluid; Microstructure.*

1. Introduction

Biodegradable materials with adequate load-bearing capacity and biocompatibility are presently important study areas in the biomedical field for temporary implants. The toxic nature of metallic materials such as stainless steel, iron-based alloys, titanium alloys, etc., in physiological environments is the most significant constraint, as is their fast degradation [1, 2]. Magnesium-based alloys with suitable compositions and surface treatments can be employed as implant materials for temporary implants. Magnesium alloys have characteristics that are almost identical to natural bone, such as density and Young's modulus, making them more suitable for application as biodegradable biomaterials. The characteristics of magnesium alloys also prohibit stress shielding in implants. Mg, a vital and inherent element in the human body, may degrade and be absorbed when new bone grows, eliminating the need for surgical removal. Mg alloys exhibit excellent osteoinductivity, which promotes bone repair through boosting osteoblast activity and bio-mineralization [3-5]. However, implants made up of Mg and its alloys degrade faster in physiological environments than the usual healing process, it is because of its strong reactivity, Mg is extremely prone to degradation. The porosity and brittleness of the surface oxide layer limit its ability to protect against degradation, particularly in physiological/aqueous environment containing chloride ions. Nonetheless, the high degradation rate (DR) of Mg alloy in the physiological/aqueous environment is a significant obstacle to the successful development of biodegradable implants because it loses the mechanical strength necessary for biomedical implant support [6, 7]. Alloying, surface treatment and mechanical working are needed to control Mg degradation at a pace that corresponds with tissue growth. Surface coatings can also play significant role to reduce the initial rapid degradation rate, preventing early implant failure prior to full bone healing [8, 9].

Mg-Zn-RE-Zr alloy is a unique set of magnesium alloys with excellent performance characteristics owing to alloying additions. The alloying of Zinc (Zn) in Mg improves both mechanical characteristics and corrosion resistance [2]. The solid solution of Zn in Mg can improve corrosion resistance by increasing the electrode potential of the α-Mg matrix, which is higher than pure Mg [10]. Rare earth metals exhibit superior castability, fine grain structure, increased strength, and improved anti-corrosion properties [11]. Zirconium (Zr), specifically, is added to magnesium because it has the highest effect on grain refinement in magnesium alloys [12]. In recent years, more attention has been paid to the ZE41A alloy, which belongs to the aforementioned group, because the cast alloy has low micro-porosity, good machinability, and corrosion resistance [13, 14]. However, the application of this alloy is limited by its low mechanical properties at room temperature, particularly poor ductility caused by the production of a brittle ternary phase on the grain boundaries [15]. Wu et al. [16] reported that the addition of a nano-hydroxyapatite coating with friction stir processing on WE43 Mg alloy has an improved micro-hardness along with enhanced corrosion resistance. A study of ZE41A Mg alloy reported that a coating of WC-Cu powder increased the micro-hardness of the alloy at low compaction load with a partially sintered electrode [17]. Another study of ZE41 Mg alloy ball burnished at loads of 40 to 80 N revealed that at the load of 60 N, the highest micro-hardness was achieved with an increase of 35.5% as compared to the unburnished sample [18]. A mechanical research found that the Mg-2Zn-1Ca (ZX21) alloy has good mechanical properties, including an ultimate tensile strength of 283 MPa and a failure elongation of 29% due to recrystallization and grain refining by Ca [19]. HA is a significant mineral in the cartilage of bones, and it is highly biocompatible and biologically active. HA's intrinsic brittleness and poor fracture toughness prevent it from supporting considerable loads, but it can be employed as a covering for other load-bearing biomaterials [9, 20]. In a degradation investigation of the Mg-1Zn-1Gd (ZG11) alloy, Li et al. [21] observed that the generated HA layer efficiently covered the implant surface's microholes and microcracks. In a study of HA-coated pure Mg alloy, Kim et al. concluded that HA-coated samples had a reduced corrosion rate compared to pure Mg in SBF. HA coating also results in the improvement of in vitro and in vivo biocompatibilities [22]. Kumar et al. [23] optimized CNC milling process parameters of ZE41A Mg alloy to investigate their effects on degradation rate after 7 days of immersion in SBF and found that at optimized parameter settings surface roughness and degradation rate both reduced.

Non-traditional machining, such as WEDM, is beneficial to improve surface characteristics of Mg alloys at optimal parametric settings, hence reducing degradation rate and improving their mechanical characteristics. Surface and subsurface properties change during WEDM processing, affecting the mechanical properties and degradation rate of Mg alloys [24]. PMWEDM is a hybrid technique that uses powder in the dielectric to improve surface smoothness and assist in lowering degradation rate. There was no investigation of PMWEDM and HA coatings on ZE41A Mg alloy to determine their impact on microstructure and micro-hardness following immersion in SBF. In this experiment, the microstructure and micro-hardness of ZE41A alloy were examined before and after 14 days of immersion in SBF.

2. Materials and Experimental Method

2.1 Work Material

Experiments have been conducted on as cast ZE41A Mg alloy samples of size 12×12×4 mm. A fine zinc metal powder has been used for the purpose of PM-WEDM. Zinc metal powder with 99% purity and mesh size 300 has been mixed with de-ionized water. Zn powder was taken with a concentration of 3g/l. Table 1 represents the physical, mechanical and thermal properties of ZE41A Mg alloy. The elemental composition of the ZE41A magnesium alloy is detailed in table 2. The sample surface was characterized by using a field emission scanning electron microscope (FESEM) (JEOL model JSM-7610F Plus).

Table 1. Properties of ZE41A Mg alloy

Properties	Value in metric
Ultimate Tensile Strength (UTS)	205-210 MPa
Yield Strength	140-145 MPa
Compressive Strength	340-350 MPa
Brinell Micro-hardness (as cast)	62-65 HB
Vickers Micro-hardness (as cast)	65-72 HV
Elongation	3.50 %
Modulus of Elasticity	44.12 GPa
Density	1.84 g/cm^3
Thermal Expansion Coefficient (α)	27 µm/mºC
Grain Size (as cast)	78-82 µm

Table 2. Elemental composition of ZE41A Mg alloy

Element	Zinc (Zn)	Zirconium (Zr)	Rare Earth Materials (REEs)	Manganese (Mn)	Copper (Cu)	Nickel (Ni)	Magnesium (Mg)
% content	3.5-5	0.4-1	0.75-1.8	0.15	0.10	0.010	91.5-95

2.2 Experimental Set-Up

Experiments have been done with ZE41A Mg alloy on the Electronica ELPULS 40A DLX Sprint-cut CNC WEDM installed at Guru Jambheshwar University of Science and Technology, Hisar, using a soft brass wire electrode with a 0.25 mm diameter. The input parameters taken for PMWEDM were peak current (70 ampere), pulse on time (0.15 micro second), pulse of time (26 micro second) and servo voltage (30 volts). The de-ionized (DI) water and Zn metal powder mixture was used as a dielectric fluid. Figure 2 (a) & (b) shows the schematic diagram of the experimental setup of PM-WEDM and a separate tank of 100-litre capacity, respectively.

Figure 1. Electronica ELPULS 40A DLX Sprint-cut CNC WEDM machine

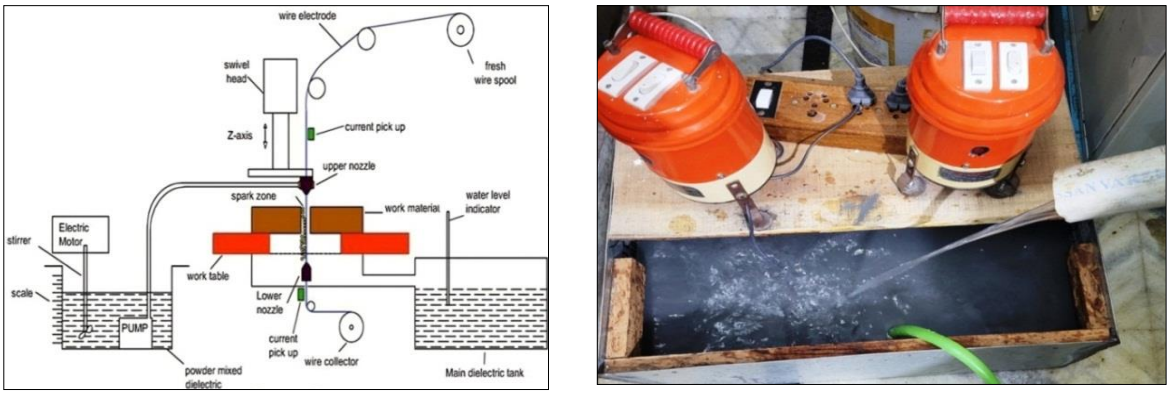

(a) (b)

Figure 2. Schematic diagram of the experimental setup of PM-WEDM [32] and separate tank to supply powder-mixed dielectric fluid

2.3 HA Coating and Immersion Study

The electrochemical deposition (ECD) technique was used to deposit HA coating on ZE41A Mg alloy in an aqueous solution, which was subsequently dried at room temperature. Coating was produced using mechanically polished samples and abrasive sheets with grit sizes of 200, 400, 600, 1000, 1500, and 2000. The samples were then ultrasonically cleaned in acetone at room temperature for 10 minutes before being air-dried. During ECD coating, the samples served as the cathode (+ve) and a platinum strip as the anode (-ve) as an inert material. A current of 0.2 amps was transmitted at a constant voltage of 3.5 volts, while the electrolyte was constantly stirred at 200 rpm. The coating layer developed was di-calcium phosphate di-hydrate, also known as brushite ($CaHPO_4.2H_2O$), a weak and unstable calcium phosphate (CaP) coating [25]. To achieve a more stable phase of HA [$Ca_{10}(PO_4)_6(OH)_2$], an alkaline treatment (acid-base reaction) is necessary, converting brushite to hydroxyapatite. The deposited samples were immersed in a 1 M NaOH solution at 80ºC for 2 hours [26, 27]. The samples were placed in simulated body fluid (SBF) prepared according to the standard given by Kokubo et al. [28], while maintaining a pH of 7.4 [29]. The degradation of Mg alloys is time dependent, with the highest corrosion or degradation occurring during the first week of immersion in SBF [30], since after one week, a passive layer forms, slowing down the degradation rate. In this experimental study, the parent, PMWEDMed, and HA-coated samples were immersed in SBF for 14 days. Experimental set-up of Vickers micro-hardness tester and sample mounted on tester is shown in figure 3. Samples were immersed in SBF using polystyrene bottles held within the BOD incubator in 95% air, 5% CO_2 at 37 ± 1.5°C for 14 days. The amount of SBF for various Mg samples was determined using the SBF-to-surface-area ratio of 0.20 mL/mm² [31].

2.4 Microstructure and Micro-hardness

Microstructure of parent, machined and coated samples was analyzed by using FESEM. Surface geometries and properties are important for forecasting the corrosion behavior of magnesium alloys, as surface degradation is closely related to mechanical performance. Micro-hardness of samples was calculated with Vickers Micro-hardness tester (INNOVA TEST FALCON 450) by taking force of 200gm and dwell time of 10 sec. Set-up of Vickers micro-hardness tester and sample mounted on tester table is shown in figure 3. Results were automatically drawn by micro-hardness tester after calculating average diagonal. Formula for Vickers micro-hardness is given below in (1):

$$\text{Vickers Micro-hardness} - \frac{1854.4 \times F}{d \times d} \text{ HV} \qquad (1)$$

Where, F = force applied in gmf and d = mean diagonal in µm, [d = (d1 + d2) / 2, d1 & d2 are two diagonals]

Figure 3. Vickers micro-hardness tester and sample mounted

3. Results and Discussion

3.1 Powder Mixed Machining and HA coating influence on Microstructure and Micro-hardness

FESEM imaging was used to analyze the surface properties and structures of the parent, PMWEDMed, and HA-coated samples. The images also aid in understanding the degradation behavior of these alloy samples, as surface characteristics have a direct impact on alloy degradation. Implant materials with high surface roughness have poor degradation resistance, which is caused by high temperature generation on the sample's surface at the point of contact with the wire electrode. After the high temperature created during machining, the dielectric medium serves as a flushing medium and coolant. This rapid heating and cooling impact increases surface roughness [32]. FESEM images of surface microstructure of Mg alloys were shown in figure 4 (a)-(c). Figure 4 (a) depicts the surface structure of the parent Mg alloy; no microcracks were seen on the surface. A few microholes and small craters were found, which might have been generated by temperature changes during the WEDM process. Oxide layers were present on the surface of the parent sample as a result of Mg interaction with oxygen, as well as abrasive layers formed during sample polishing on abrasive sheets. Figure 4 (b) shows presence of large number of microholes and microcracks, again produced due to high temperature difference and high spark energies. During WEDM process when trapped gases try to escape from molten metal creates large globules finally resulting in large craters after bursting, these craters promotes degradation rate [33, 34]. Shiny zinc particles were also visible, as shown in figure 4 (b), which were accumulated while machining with PMWEDM. HA-coated samples showed no microcracks and had small craters. The number of microholes was also negligible; instead, CaP particles can be seen as shown in figure 4(c). This layer of CaP HA particles filled the microcracks and microholes, providing a barrier layer to improve surface finish and inhibit degradation rates.

Table 3 shows the computed Vickers MH values of test samples before immersion, which were performed at 200 gmf force and a dwell period of 10 seconds. The results show that PMWEDM machining and HA coating methods improve the MH of Mg samples as compared to parent samples. The MH of PMWEDMed samples rose due to modest heat treatment from heating and cooling reactions. It may also be raised due to the accumulation of zinc particles on the sample surface, which improves surface mechanical properties and degradation resistance [2, 35]. The HA coating formed a layer of CaP, which increased the MH of the samples and, as a result, their degradation resistance. MH of parent, PMWEDMed and HA coated samples (in 2 numbers) was shown in figure 5. The value of Vickers MH of Mg alloys treated with PMWEDM and HA coating increased to a value of (for sample 1/2) 74.67/72.67 HV and 70.67/70.33 HV, respectively, while MH of parent samples was recorded as 67/67.33 HV.

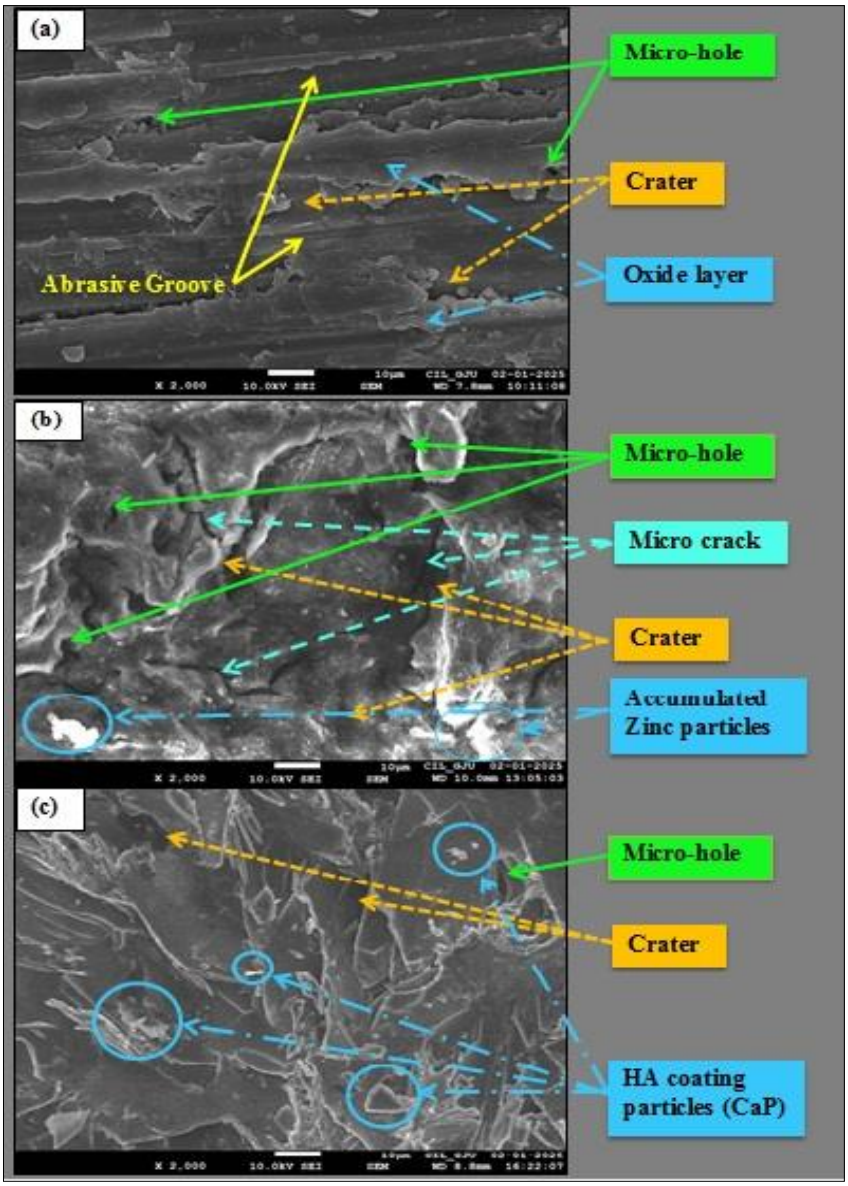

Figure 4. SEM images of surface microstructure of (a) parent, (b) PMWEDMed and (c) HA coated samples before immersion

Table 3. Vickers Microhardness results before immersion

Sample Name	Applied Force (in gmf)	Time Interval/Dwell time (in sec)	Vicker's Hardness (in HV) before immersion	Average Vicker's Hardness (in HV) before immersion
Parent 1	200	10	67	67.17
Parent 2	200	10	67.33	
PMWEDM 1	200	10	74.67	73.67
PMWEDM 2	200	10	72.67	
HA Coated 1	200	10	70.67	70.5
HA Coated 2	200	10	70.33	

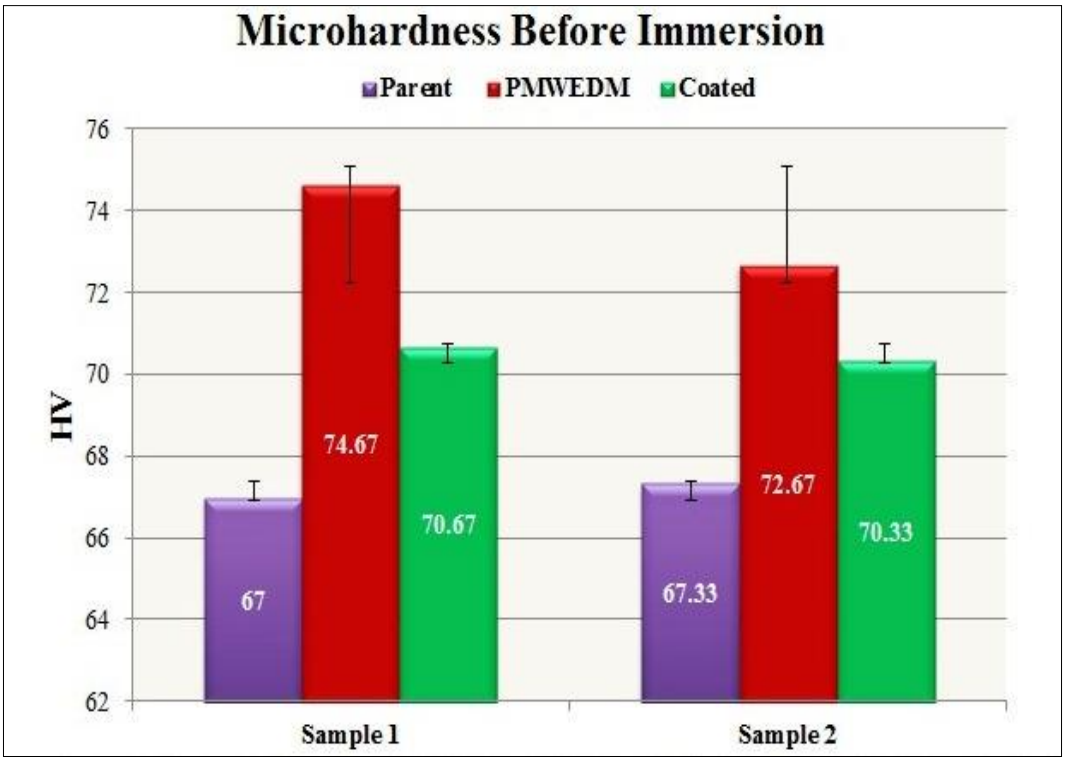

Figure 5. Vickers Micro-hardness of parent, PMWEDMed and HA coated samples before immersion

3.2 Microstructure and Immersion Study Influence on Micro-hardness

Figure 6 depicts samples after 14 days of immersion in SBF. The photos of the samples demonstrate that the surface topographies of all three samples were almost identical owing to degradation. Figure 6(b) shows large microholes and pits formed by degradation on the surface of the PMWEDMed sample, whereas Figure 6(a) shows pits and microholes that are much smaller. HA-covered samples displayed less uneven topography than PMWEDMed samples. Vickers MH was then evaluated on the degraded samples using the same settings (force - 200 gmf and dwell period - 10 seconds). Figure 7 shows the Vickers Micro-hardness of parent, PMWEDMed and HA coated samples before and after 14 days immersion with % loss trend. The MH findings for tested samples are shown in table 4 of immersed samples. The MH of parent materials reduced to 57 HV from 67.17 HV, representing a 14.93 percent decline. This loss is due to surface ruptures in the parent sample during the immersion phase. The MH of PMWEDMed samples determined after immersion was 60 HV, compared to 73.67 HV before immersion. The PMWEDMed sample had the largest loss of MH following immersion, with a percentage loss of 19.62. It was because of the high degradation rate of PMWEDMed samples during immersion. Large surface irregularities caused SBF to penetrate the alloy's surface more deeply, resulting in high weight loss [34]. A loss of 11.79% of MH was recorded for HA-coated samples, whose MH was decreased from 70.5 HV to 62.33 HV. The coated sample shows the lowest MH loss after immersion because of its smooth surface and the formation of a CaP layer, which controls the degradation of Mg alloy.

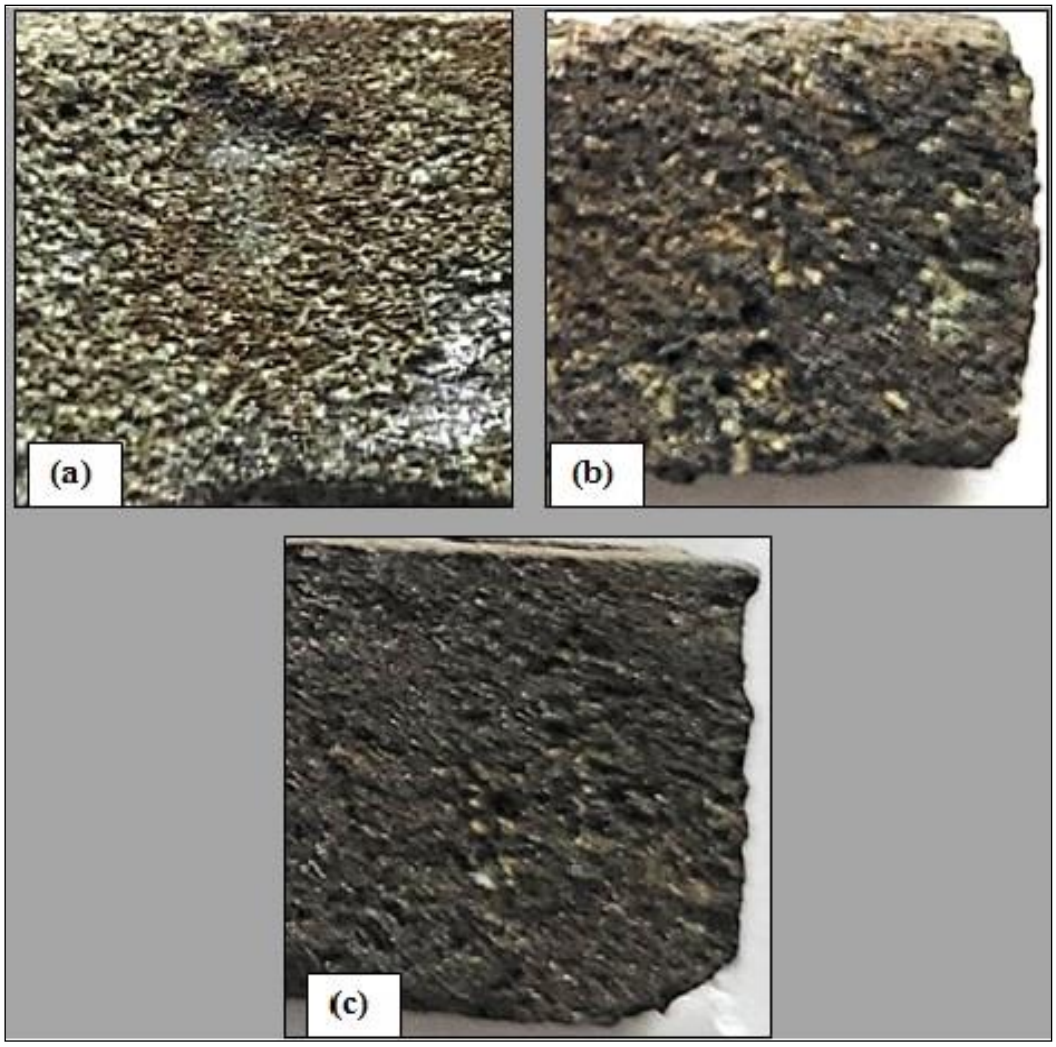

Figure 6. Images of (a) parent, (b) PMWEDMed and (c) HA coated samples after 14 days immersion in SBF

Table 4. Vickers Microhardness before and after 14 days immersion with % loss

Sample Name	Applied Force (in gmf)	Time Interval/Dwell time (in sec)	Vicker's Hardness (in HV) before immersion	Vicker's Hardness (in HV) after 14 days immersion	% loss of Microhardness after 14 days immersion
Parent	200	10	67.17	57	14.93
PMWEDM	200	10	73.67	60	19.65
HA Coated	200	10	70.5	62.33	11.79

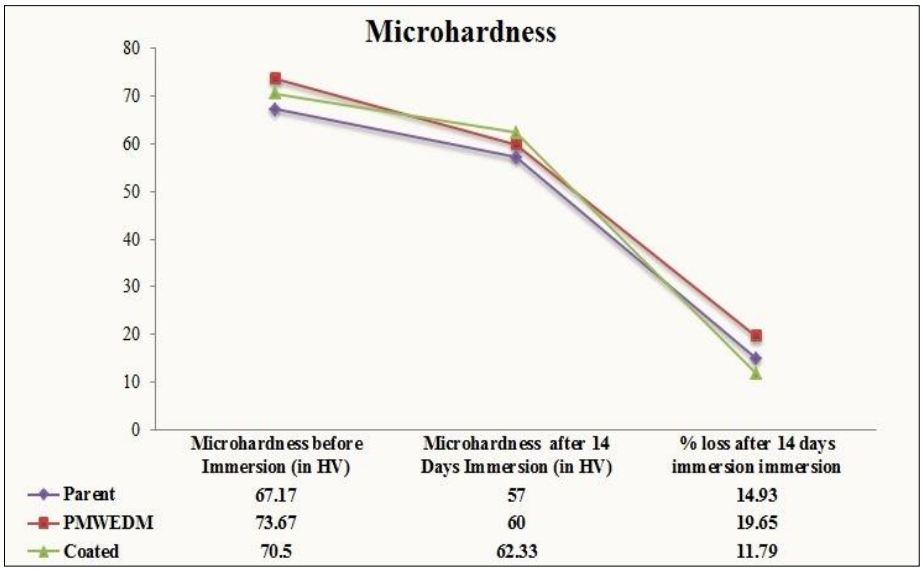

Figure 7. Vickers Micro-hardness of parent, PMWEDMed and HA coated samples before and after 14 days immersion with % loss

4. Conclusions

Experiments were carried out to investigate the effects of PMWEDM and HA coating on the surface microstructure and micro-hardness of the ZE41A magnesium alloy. FESEM imaging was used to investigate surface microstructures. The parent, PMWEDMed, and coated Mg samples were immersed in SBF for 14 days, and the Vickers micro-hardness tester was used to calculate the MH of the Mg samples before and after immersion. Vickers' MH findings before immersion demonstrated that the PMWEDM technique and HA coating improve the MH of ZE41A Mg samples as compared to the bare parent samples. After immersion in SBF, Vickers' findings indicated that PMWEDMed samples display the highest loss of MH as compared to parent and coated samples. The computed loss for PMWEDMed samples was 19.65%, whereas that for parent and HA-covered samples was 14.93% and 11.79%, respectively. It may be inferred that HA coating may aid in increasing the surface and micro-hardness characteristics of Mg alloys. The PMWEDM technique can also be used with different parameter settings by taking other powders at varying concentrations.

Funding

The authors declare that there is no source of funding.

Conflict of interest

The authors declare that there are no conflicts of interest.

References

[1] Sezer, N., Evis, Z., Kayhan, S.M., Tahmasebifar, A. and Koç, M., 2018. Review of magnesium-based biomaterials and their applications. *Journal of magnesium and alloys*, *6*(1), pp.23-43.

[2] Kumar, S. and Katyal, P., 2022. Factors affecting biocompatibility and biodegradation of magnesium based alloys. *Materials Today: Proceedings*, *52*, pp.1092-1107.

[3] Vasu, C., Venkateswarlu, B., Rao, R.V., Chanti, B., Saikrishna, M. and Sunil, B.R., 2019. Microstructure, mechanical and corrosion properties of friction stir processed ZE41 Mg alloy. *Materials Today: Proceedings*, *15*, pp.50-56.

[4] Liu, C., Ren, Z., Xu, Y., Pang, S., Zhao, X. and Zhao, Y., 2018. Biodegradable magnesium alloys developed as bone repair materials: a review. *Scanning*, *2018*(1), p.9216314.

[5] Zhenkang, W.E.N., Lei, L.E.I., Zhang, H., Zheyu, J.I.N., Zhengming, S.H.A.N., Weiyang, L.I.U., Wenxue, T.O.N.G., Jiankun, X.U. and Ling, Q.I.N., 2025. Magnesium-containing implants enhance bone healing: A mechanobiological perspective. *Mechanobiology in Medicine*, p.100161.

[6] Cho DH, Lee BW, Park JY, Cho KM, Park IM. Effect of Mn addition on corrosion properties of biodegradable Mg-4Zn-0.5 Ca-xMn alloys. Journal of Alloys and Compounds. 2017 Feb 25;695:1166-74.

[7] Peng G, Qiao Q, Jin L, Zhang B, Wang Y, Huang K, Yao Q, Zhang D, Zhang Z, Fang T, Wu J. A novel CeO2/MgAl2O4 composite coating for the protection of AZ31 magnesium alloys. Journal of Materials Science. 2020 Feb;55(4):1727-37.

[8] Gao J, Su Y, Qin YX. Calcium phosphate coatings enhance biocompatibility and degradation resistance of magnesium alloy: Correlating in vitro and in vivo studies. Bioactive Materials. 2021 May 1;6(5):1223-9.

[9] Guan RG, Johnson I, Cui T, Zhao T, Zhao ZY, Li X, Liu H. Electrodeposition of hydroxyapatite coating on Mg-4.0 Zn-1.0 Ca-0.6 Zr alloy and in vitro evaluation of degradation, hemolysis, and cytotoxicity. Journal of Biomedical Materials Research Part A. 2012 Apr;100(4):999-1015.

[10] Vanýsek, P., 2012. Electrochemical series. *Handbook of chemistry and physics*, *93*, pp.5-80.

[11] Bryła, K., 2020. Microstructure and mechanical characterisation of ECAP-ed ZE41A alloy. *Materials Science and Engineering: A*, *772*, p.138750.

[12] Gupta, M. and Sharon, N.M.L., 2011. Corrosion Aspects of Magnesium-Based Materials. *Magnesium, Magnesium Alloys, and Magnesium Composites; John Wiley & Sons, Inc*, pp.207-231.

[13] Baral, S.K., Thawre, M.M., Sunil, B.R. and Dumpala, R., 2023. A review on developing high-performance ZE41 magnesium alloy by using bulk deformation and surface modification methods. *Journal of Magnesium and Alloys*, *11*(3), pp.776-800.

[14] AbdelGawad, M., Usman, C.A., Shunmugasamy, V.C., Karaman, I. and Mansoor, B., 2022. Corrosion behavior of Mg-Zn-Zr-RE alloys under physiological environment–impact on mechanical integrity and biocompatibility. *Journal of Magnesium and Alloys*, *10*(6), pp.1542-1572.

[15] Ding, R., Chung, C., Chiu, Y. and Lyon, P., 2010. Effect of ECAP on microstructure and mechanical properties of ZE41 magnesium alloy. *Materials Science and Engineering: A*, *527*(16-17), pp.3777-3784.

[16] Wu, B., Yusof, F., Li, F., Miao, H., Bushroa, A.R., Muhamad, M.R.B., Badruddin, I.A. and Ibrahim, M.Z., 2024. Effects of friction stir processing and nano-hydroxyapatite on the microstructure, hardness, degradation rate and in-vitro bioactivity of WE43 alloy for biomedical applications. *Journal of Magnesium and Alloys*, *12*(1), pp.209-224.

[17] Elaiyarasan, U., Satheeshkumar, V. and Senthilkumar, C., 2020. Effect of sintered electrode on microhardness and microstructure in electro discharge deposition of magnesium alloy. *Journal of the Mechanical Behavior of Materials*, *29*(1), pp.69-76.

[18] Baral, S.K., Thawre, M.M., Sunil, B.R. and Dumpala, R., 2025. Effect of Burnishing Load on Surface Roughness and Wear Behaviour of ZE41 Magnesium Alloy. *Archives of Metallurgy and Materials*, pp.1019-1025.

[19] Zareian, Z., Emamy, M., Malekan, M., Mirzadeh, H., Kim, W.J. and Bahmani, A., 2020. Tailoring the mechanical properties of Mg–Zn magnesium alloy by calcium addition and hot extrusion process. *Materials Science and Engineering: A*, *774*, p.138929.

[20] Zhou, H. and Lee, J., 2011. Nanoscale hydroxyapatite particles for bone tissue engineering. *Acta biomaterialia*, *7*(7), pp.2769-2781.

[21] Li, X., Lin, E., Wang, K., Ke, R., Kure-Chu, S.Z. and Xiao, X., 2024. Fabrication and characterization of hydroxyapatite coatings on anodized magnesium alloys by electrochemical and chemical methods intended for biodegradable implants. Ceramics International, 50(19), pp.36838-36848.

[22] Kim, S.M., Jo, J.H., Lee, S.M., Kang, M.H., Kim, H.E., Estrin, Y., Lee, J.H., Lee, J.W. and Koh, Y.H., 2014. Hydroxyapatite-coated magnesium implants with improved in vitro and in vivo biocorrosion, biocompatibility, and bone response. Journal of Biomedical Materials Research Part A: An Official Journal of The Society for Biomaterials, The Japanese Society for Biomaterials, and The Australian Society for Biomaterials and the Korean Society for Biomaterials, 102(2), pp.429-441.

[23] Kumar, R., Katyal, P. and Kumar, K., 2023. Effect of end milling process parameters and corrosion behaviour of ZE41A magnesium alloy using Taguchi based GRA. Biointerface Res. Appl. Chem, 13(3), p.214.

[24] Denkena, B., Lucas, A., Thorey, F., Waizy, H., Angrisani, N. and Meyer-Lindenberg, A., 2011. Biocompatible magnesium alloys as degradable implant materials-Machining induced surface and subsurface properties and implant performance. Special issues on magnesium alloys, pp.109-127.

[25] Mahmud, S., Rahman, M., Kamruzzaman, M., Khatun, H., Ali, M.O. and Haque, M.M., 2023. Recent developments in hydroxyapatite coating on magnesium alloys for clinical applications. *Results in Engineering*, *17*, p.101002.

[26] Wang, H.X., Guan, S.K., Wang, X., Ren, C.X. and Wang, L.G., 2010. In vitro degradation and mechanical integrity of Mg–Zn–Ca alloy coated with Ca-deficient hydroxyapatite by the pulse electrodeposition process. *Acta biomaterialia*, *6*(5), pp.1743-1748.

[27] Antoniac, I., Miculescu, F., Cotrut, C., Ficai, A., Rau, J.V., Grosu, E., Antoniac, A., Tecu, C. and Cristescu, I., 2020. Controlling the degradation rate of biodegradable Mg–Zn-Mn alloys for orthopedic applications by electrophoretic deposition of hydroxyapatite coating. *Materials*, *13*(2), p.263.

[28] Kokubo, T. and Takadama, H., 2006. How useful is SBF in predicting in vivo bone bioactivity?. *Biomaterials*, *27*(15), pp.2907-2915.

[29] Taltavull, C., Shi, Z., Torres, B., Rams, J. and Atrens, A., 2014. Influence of the chloride ion concentration on the corrosion of high-purity Mg, ZE41 and AZ91 in buffered Hank's solution. *Journal of Materials Science: Materials in Medicine*, *25*(2), pp.329-345.

[30] Jiang, J., Zhang, F., Ma, A., Song, D., Chen, J., Liu, H. and Qiang, M., 2015. Biodegradable behaviors of ultrafine-grained ze41a magnesium alloy in dmem solution. *Metals*, *6*(1), p.3.

[31] Singh, N., Batra, U., Kumar, K. and Mahapatro, A., 2021. Investigating TiO2–HA–PCL hybrid coating as an efficient corrosion resistant barrier of ZM21 Mg alloy. *Journal of Magnesium and Alloys*, *9*(2), pp.627-646.

[32] Kumar V, Sharma N, Kumar K, Khanna R. Surface modification of WC-Co alloy using Al and Si powder through WEDM: A thermal erosion process. Particulate Science and Technology. 2018 Oct 3;36(7):878-86.

[33] Nguyen, H.P., Banh, T.L. and Van, T.N., 2024. Optimization of PMEDM Process Parameters for MRR, TWR, RA, and HV Using Taguchi Method and Grey Relational Analysis for Die Steel Materials. In *Decision-Making Models and Applications in Manufacturing Environments* (pp. 211-244). Apple Academic Press.

[34] Chakraborty, S., Mitra, S. and Bose, D., 2022. Optimisation of machining performance in PMWEDM of titanium alloy using the hybrid technique (GRA-PCA). *Advances in Materials and Processing Technologies*, *8*(2), pp.1467-1480.

[35] Kumar, R. and Katyal, P., 2022. Effects of alloying elements on performance of biodegradable magnesium alloy. *Materials Today: Proceedings*, *56*, pp.2443-2450.